Thick, three-dimensional nanoporous density-graded materials formed by optical exposures of photopolymers with controlled levels of absorption

Yun-Suk Nam,[1] Seokwoo Jeon,[1] Daniel Jay-Lee Shir,[1] Alex Hamza,[2] and John A. Rogers[1,3,*]

[1]Department of Materials Science and Engineering, University of Illinois at Urbana/Champaign, 1304 Green Street, Urbana, 61801, USA
[2]Lawrence Livermore National Laboratory, 7000 East Avenue, Livermore, California 94550, USA
[3]Frederick Seitz Materials Research Laboratory, 104 South Goodwin Avenue Urbana, Illinois 61801, USA

*Corresponding author: jrogers@uiuc.edu

Three-dimensional (3D) intensity distributions generated by light passing through conformal phase masks can be modulated by the absorption property of photosensitive materials. The intensity distributions have extremely long depth of focus, which is proportional to the size of the phase masks, and this enables one to pattern thick ($\sim 100\ \mu m$), nanoporous structures with precise control of grade density. Various density-graded 3D structures that result from computational modeling are demonstrated. Results of x-ray radiograph and the controlled absorption coefficient prove the dominant mechanism of the generated graded density is absorption of the photosensitive materials. The graded-density structures can be applied to a chemical reservoir for controlled release of chemicals and laser target reservoirs useful to shape shockless wave compression.   © 2007 Optical Society of America

OCIS codes: 220.4000, 320.7110, 050.0050.

1. Introduction

Materials with controlled gradients in density are of interest for many potential applications, ranging from superrefractory materials [1], to impact resistant materials [2], and many others [3]. Polymeric density-graded structures (DGS) can be used directly in some of these applications or they can serve as templates for growth or deposition of other materials. These polymer structures typically use porosity to achieve effective gradients in density, in which the pore size and/or spacing varies continuously with position. The fabrication is often accomplished with controlled drying [4], or an electrochemical process [5]. A limitation of these approaches is that they provide little flexibility in the control over functional forms for the gradients and for the microstructural and nanostructural features of the materials that give rise to the gradients. In addition, many of the methods are not easily scaled to large areas or large sample quantities. A relatively new type of experimentally simple, optical method for three-dimensional (3D) patterning of photosensitive polymers and other materials has potential applications in the area of DGS materials. This method, which we refer to as proximity field nanopatterning (PnP) [6–9] due to its use of optical intensity distributions that form in proximity to a diffractive phase mask, can generate highly periodic 3D structures in photosensitive materials through optical exposures with a coherent or substantially incoherent source of light. The sizes of the patterned areas are only limited by the sizes of the phase masks and the illumination areas. A wide range of structure geometries are possible by controlling the mask layouts, the properties of the exposure light (e.g., wavelengths and wavelength bandwidths, coherence, exposure angles, etc.), and by the nature of the interaction between the light and the photosensitive material (e.g., single-photon or multiphoton effects) [6–9]. In a recent report [7], we demonstrated the possibility for

generating nanoporous structures with systematically varying pore sizes through the thickness of thin (5–10 μm) films by controlling the angular and spectral bandwidth of the exposure source. Although such techniques work well for thin films, they are not useful for generating the sorts of relatively thick (e.g., up to 100 μm) material systems that are required by many applications. The challenges in this case are associated with small, residual levels of optical absorption that frustrate the formation of the gradient profiles. This paper describes a different strategy for DGS fabrication by PnP that avoids this problem by exploiting engineered levels of optical absorption in the photopolymer. This approach is fundamentally different than previous work in the sense that the structure control is provided by the design of the photosensitive material, rather than by the phase masks or the exposure conditions. The resulting method is important because it provides new forms of flexibility in control over the PnP process that, for the example illustrated here, enable the fabrication of thick DGS films in simple, single exposure steps. This paper describes the materials and optical aspects of this method. Computational results, x-ray radiographs, and results obtained with photopolymers designed with different optical extinction coefficients illustrate the essential features. As a representative application example, we use optimized DGS structures as a model system for controlled chemical release of riboflavin. Here, the DGS acts as a host that affects the release of riboflavin with kinetics that are controlled by the nature of the gradients in the nanoscale porosity of the structure.

2. Experimental Setup

Figure 1 illustrates the exposure configuration. The substrate consists of a 0.13 mm thick glass coverslip coated with a thick (up to 100 μm), spin cast layer of a transparent epoxy photopolymer (EPON SU-8-50, Microchem Corp., Newton, MA, USA). A previously
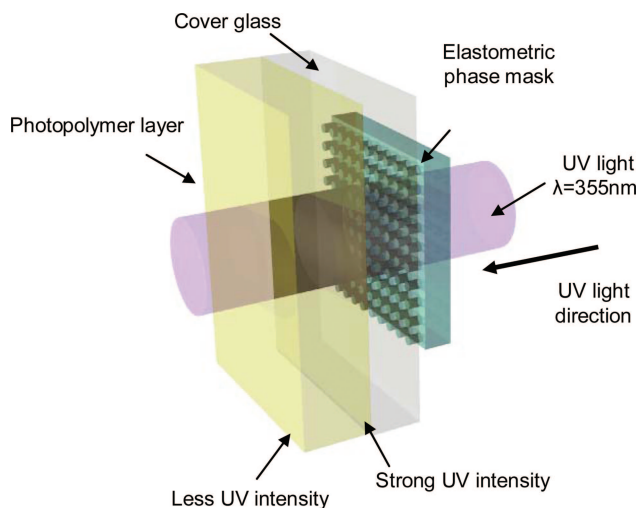
deposited thin, fully cured layer of this material (~5 μm SU-8) serves as an adhesion promoter to ensure good bonding of the thick layer to the underlying support. All of the optics for the exposure are built into a single soft, conformable phase mask element, formed by casting and curing prepolymers to the elastomer poly(dimethylsiloxane) (PDMS) [6] or perfluoropolyether (PFPE) [10,11] against high-resolution patterns defined by projection mode photolithography. Placing this mask on the back side of the coverslip leads to conformal contact, driven by generalized adhesion forces between the mask and substrate [12]. This procedure represents the optical alignment step. Exposure occurs by shining ultraviolet light (UV; $\lambda = 355$ nm, $\phi = 0.25$ in.) through the phase mask to create a 3D distribution of intensity near the surface of the mask, as well as in proximity to it, through the entire thickness of the epoxy material. The laser power is ~0.7 mW with a beam diameter of ~6 mm, and an exposure time of 16 s. This exposure, followed by washing away of the unexposed regions of the photopolymer generates a solid polymer structure in the geometry of the intensity distribution. In previous examples, these exposures occurred with the photopolymer in direct contact with the mask [6–9]. Also, the optical properties of the photopolymer (other than its index of refraction) were designed specifically not to strongly influence the geometry of the resulting structures.

The "back side" exposure method illustrated in Fig. 1, which is enabled by the large depth of focus of PnP, combined with chemical control of optical absorption in the photopolymer represent the key aspects of the fabrication approach introduced here. In this configuration, the region of the photopolymer near the surface of the substrate receives a larger exposure dose, on average, than at the air interface, due to optical losses associated with the propagation of light through the film. This optical effect leads to graded nanoporous structures with density gradients controlled by optical losses in the polymer, as described in detail in Section 3. Finite element modeling (COMSOL, Inc., Los Angeles, CA) of the optics in a simplified system reveals the essential effects.

3. Results

Figure 2 shows results for the flow of light through a phase mask and into media (index of refraction, $n = 1$) with three different levels of optical absorption. The mask consists of raised and recessed lines of binary relief (depth: 420 nm; linewidths and spaces: 300 nm) in a material with $n = 1.4$. The images on the left show the intensity distributions generated by the passage of TE polarized plane waves with a wavelength of 355 nm through the masks. Application of a binary cutoff filter located at an appropriate exposure threshold yields from these distributions a simulation of structures that would result from exposure and development. These calculations predict a periodic modulation in the intensity and a corresponding uniformly periodic solid structure (i.e., depth and position independent pore size) for the case of zero light

Fig. 1. (Color online) Schematic of an optical phase mask approach to fabricating density graded 3D nanoporous polymer structures.
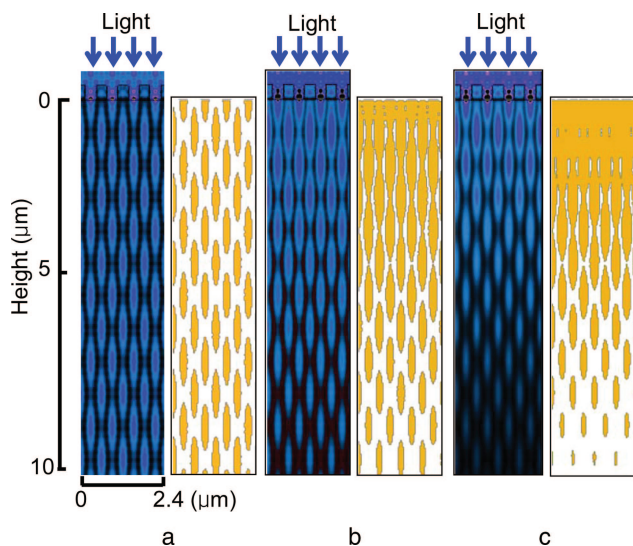
Fig. 2. (Color online) Finite element modeling of intensity distributions (blue, left) and structures in SU-8 with proper cutoff filters (yellow, right) associated with optical exposures (wavelength = 355 nm) through phase masks gratings with wavelengths, D = 600 nm, and depths of relief, RD = 420 nm. The index of the mask material and the surroundings is 1.4 and 1, respectively. Intensity distributions for the cases of optical absorption in the surrounding are a, 0%; b, 20%; and c, 35%.

Fig. 3. (Color online) DGS generated from a PFPE phase mask with a hexagonal array of cylindrical posts of relief, with relief depth, RD = 420 nm; diameters, D = 460 nm; and period, P = 600 nm. a, Optical image of a DGS film on a cover glass. b, c, Scanning electron micrographs of these structures. The effective density varies by nearly a factor of ten from the bottom to the top.

absorption in the medium, as shown in Fig. 2a. By contrast, when the total absorption after light passing through the sample is 20% (Fig. 2b) and 35% (Fig. 2c), the resulting solid structures are predicted to have a depth-dependent pore size associated with the reduction in intensity with distance from the surface of the mask. These nanoporous structures provide effective gradients in density that is set by the extent of absorption. The overall exposure dose (i.e., the position of the cutoff filter in these simulations) determines the maximum density (i.e., the size of the pores in the regions near the mask), and the absorption coefficient of the photopolymer determines the density gradient of the final structure.

Figure 3 shows optical and scanning electron microscope (SEM) images of DGS materials formed in this manner, using a PFPE phase mask. In particular, Fig. 3a presents a picture of a DGS film (thickness ~60 μm) on a cover glass; the diameter of this structure is ~6 mm, defined by the size of the laser spot used for exposure. Figures 3b and 3c present cross-sectional views of fracture surfaces of this film. As can be seen clearly in this image, the part of the film that is in contact with the substrate has the highest density (small or nonexistent pores; nearly full density), while the top surface region has relatively low density (large pores; effective density ~10× lower than the material itself). The layout of the phase mask influences the geometry of the structures. Figures 4a–4d show SEM cross-sectional views of fracture surfaces of DGS films fabricated with phase masks that present relief in the geometry of hexagonal and square arrays of cylindrical posts. X-ray radiographs (Fig. 4e) of those samples reveal
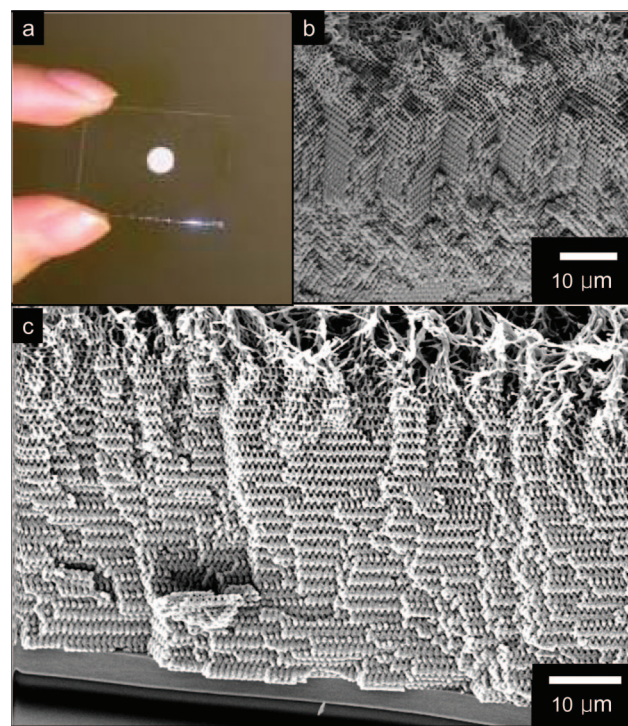
the average, depth-dependent cumulative density normal to the cross section. The intensity of the reflected signal correlates to the average density. Figure 4f shows a plot of the signal as a function of the position through the thickness of the film (red line). The calculated average intensity of light is plotted as a function of depth, normalized to the value at the surface of the film. As Fig. 4f indicates, these two quantities exhibit similar variations with depth, thereby confirming the expected mechanism for DGS formation.

The rate at which the effective density changes with depth can be controlled by adjusting the absorption. The results of Figs. 3 and 4 correspond to the intrinsic loss of the epoxy photopolymer system itself. The addition of dyes to the epoxy can increase the absorption, thereby leading to increased rates of change in density with depth. To demonstrate this capability, we used the dye tris(2,2'-bipyridyl)dichlororuthenium (II) hexahydrate (Rubpy), which strongly absorbs UV light in a wavelength range from 330 to 370 nm, as shown in Fig. 5a. The concentration of this dye in the epoxy polymer determines the absorption, as illustrated in Fig. 5(a). Figures 5b–5e present SEM images of DGSs fabricated using epoxy layers with Rubpy at concentrations of 0.0, 0.1, and 0.65 wt. % and the PFPE phase mask employed for the structures of Fig. 2. At 0 wt. %, as shown in Fig. 5b, the DGS is similar to the one in Fig. 2. With the same exposure dose, the depth
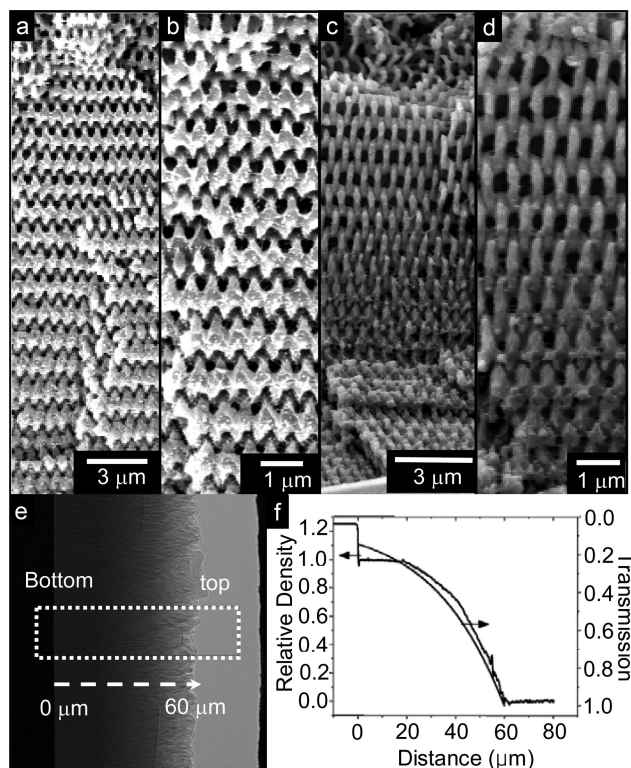
Fig. 4. a, b, Scanning electron micrographs of the nanoscale porosity associated with optically fabricated DGSs formed with a PFPE phase mask with a hexagonal array of cylindrical features of relief (relief depth, $RD = 420$ nm; diameters, $D = 460$ nm; and period, $P = 600$ nm). c, d, DGS formed with a PDMS phase mask with square array of cylindrical features of relief ($RD = 420$ nm; $D = 375$ nm, and $P = 566$ nm). e, X-ray radiograph of the cross section of a DGS structure. The gray levels reflect different effective densities. f, Plot of measured density and calculated transmission as a function of distance through the thickness of the film. A relative density of 1 corresponds to the fully cured, nonporous structure of SU-8. A relative density of 0 corresponds to a vacuum.
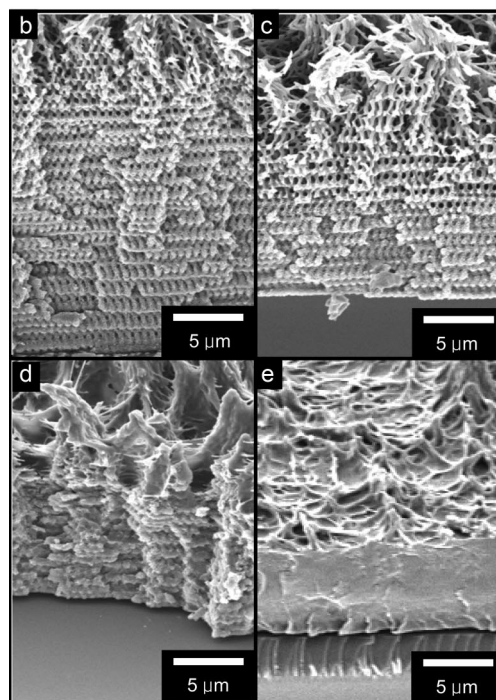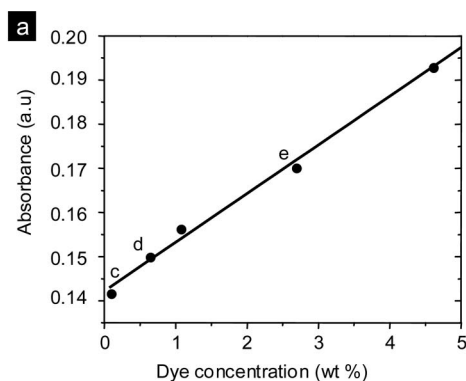

Fig. 5. a, Absorbance (arb. units) of layers of SU-8 with different concentrations of an absorbing dye. Density gradient structures fabricated from layers of SU-8 with dye concentrations of b, 0; c, 0.1; d, 0.65; and e, 2.6 wt. %.

where intensity remains strong enough to achieve interconnected 3D structures decreases. Figure 5c shows a DGS fabricated at 0.1 wt. % Rubpy. The total density variation is comparable to that of the 0 wt. % case, but the variation occurs through a total thickness of only 28 μm, instead of ∼60 μm. Figures 5d and 5e show a continuation of this trend. In all cases, the density gradient and pore size are highly reproducible and can be controlled by exposure dose and postbaking temperature and time. The method presented in this paper is relatively insensitive to environmental variations such as temperature and humidity. The high reproducibility, high tolerance to environmental variations, and simple manufacturing steps allow the possibility of mass production of thick density gradient structures.

The DGS structures presented in this paper can be used for a variety of applications, such as materials to manage shock wave propagation in laser fusion targets [13]. Here we demonstrate their implementation as host matrices for the storage and controlled release of chemicals. In this system, the chemicals, in

this case riboflavin, are loaded into the porous epoxy matrix by diffusion and capillary action, upon immersion of the structure in a solution of the riboflavin. The total pore volume defines the amount of riboflavin imbibed into the structure, for sufficiently long immersion times. Depth variations in the sizes of the pores influence the kinetics of release. Figure 6 presents a plot of the change in optical absorption at 445 nm associated with passage of light through a fluid cell that contains riboflavin B2 initially loaded into DGS. As riboflavin releases from the DGS, it diffuses into the surrounding water, and changes the measured absorption. The curve labeled "i" in Fig. 6 shows a slowly rising absorbance, associated with diffusion out of a DGS whose surface was washed immediately prior to immersion in the fluid cell. We expect that only the slowly released chemicals from the depths of the DGS affect the slow rise of absor-
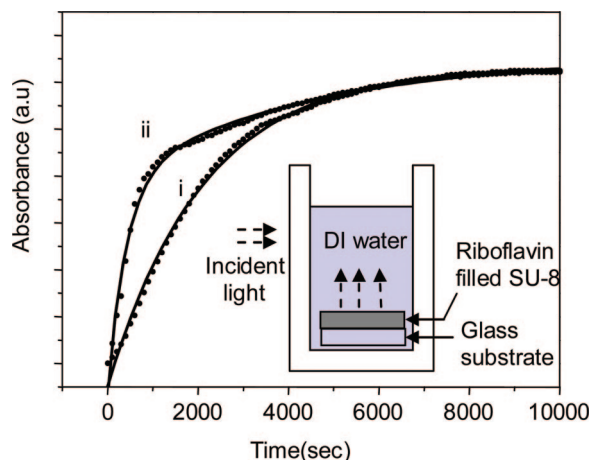
Fig. 6. (Color online) Time variation of absorbance (arb. units) measured through a fluid cell that contains a density-graded structure loaded with riboflavin (curve labeled i) and a flat surface coated with riboflavin (curve labeled ii).

bance. The curve labeled "ii" shows, for comparison, the response for the case of riboflavin adsorbed onto a flat surface. In this case, the absorbance changes quickly, due to the short diffusion path compared to the DGS case. Time constants of $\sim 2.3 \times 10^{-3}$ and $\sim 0.5 \times 10^{-3}$ s^{-1} are calculated from curves ii and i, respectively. The dependence of release kinetics on the magnitude and gradient of the porosity, with comparison to theory, is the subject of current work.

4. Conclusion

In summary, this paper introduces a simple optical method for fabricating thick nanoporous polymer films with controlled variations in pore size through the film thickness. The method for achieving nano-structured density gradient materials combines a 3D optical exposure technique with controlled levels of optical absorption in a photopolymer. Calculations, together with optical and x-ray characterization of the system, verify the key aspects of the approach. Implementation of the gradient structures as hosts for chemicals demonstrates one area of application that could have relevance to controlled drug release and catalysis.

References

1. M. Niino and S. Maeda, "Recent development status of functionally gradient materials," ISIJ Int. **30,** 699–703 (1990).
2. L.-S. Liu, Q.-J. Zhang, and P.-C. Zhai, "The optimization of propagation characteristic of elastic wave in FGM," Mater. Sci. Forum **492-493,** 453–458 (2005).
3. S. Uemura, "The activities of FGM on new application," Mater. Sci. Forum **423-4,** 1–9 (2003).
4. R. G. Frey and J. W. Halloran, "Compaction behavior of spray-dried alumina," J. Am. Ceram. Soc. **67,** 199–203 (1984).
5. R. Jedamzik, A. Neubrand, and J. Rodel, "Production of functionally graded materials from electrochemically modified carbon preforms," J. Am. Ceram. Soc. **83,** 983–985 (2000).
6. S. Jeon, J.-U. Park, R. Cirelli, S. Yang, C. E. Heitzman, P. V. Braun, P. J. A. Kenis, and J. A. Rogers, "Fabricating complex three-dimensional nanostructures with high-resolution conformable phase masks," Proc. Natl. Acad. Sci. U. S. A. **101,** 12428–12433 (2004).
7. S. Jeon, Y. S. Nam, D. Shir, and J. A. Rogers, "Three dimensional nanoporous density graded materials formed by optical exposures through conformable phase masks," Appl. Phys. Lett. **89,** 253101 (2006).
8. S. Jeon, V. Malyarchuk, J. A. Rogers, and G. P. Wiederrecht, "Fabricating three-dimensional nanostructures using two photon lithography in a single exposure step," Opt. Express **14,** 2300–2308 (2006).
9. S. Jeon, V. Malyarchuk, J. O. White, and J. A. Rogers, "Optically fabricated three-dimensional nanofluidic mixers for microfluidic devices," Nano Lett. **5,** 1351–1356 (2005).
10. T. T. Truong, R. Lin, S. Jeon, H. H. Lee, J. Maria, A. Gaur, F. Hua, I. Meinel, and J. A. Rogers, "Soft lithography using acryloxy perfluoropolyether composite stamps," Langmuir **23,** 2898–2905 (2007).
11. K. B. Wiles, N. S. Wiles, K. P. Herlihy, B. W. Maynor, J. P. Rolland, and J. M. DeSimone, "Soft lithography using perfluorinated polyether molds and PRINT technology for fabrication of 3D arrays on glass substrates," Proc. SPIE **6151,** 61513F1–61513F9 (2006).
12. Y. Y. Huang, W. Zhou, K. J. Hsia, E. Menard, J.-U. Park, J. A. Rogers, and A. G. Alleyne, "Stamp collapse in soft lithography," Langmuir **21,** 8058–8068 (2005).
13. R. F. Smith, K. T. Lorenz, D. Ho, B. A. Remington, A. Hamza, J. A. Rogers, S. Pollaine, S. Jeon, Y.-S. Nam, and J. Kilkenny, "Graded-density reservoirs for accessing high stress low temperature material states," Astrophys. Space Sci. **307,** 269–272 (2007).